Application of an Automatically Built 3D Morphometric Brain Atlas: Study of Cerebral Ventricle Shape

Gérard Subsol, Jean-Philippe Thirion and Nicholas Ayache

Institut National de Recherche en Informatique et en Automatique
Projet Epidaure
2 004, route des Lucioles, BP 93
06 902 Sophia Antipolis Cedex, France
E-mail: Gerard.Subsol@epidaure.inria.fr

Abstract. In this paper we present new results on the automatic building of a 3D morphometric brain atlas from volumetric MRI images and its application to the study of the shape of cerebral structures. In particular, we show how it is possible to define "abnormal" deformations of the cerebral ventricles with a small set of parameters.

1 Introduction

In [STA95], we presented a general method for automatically building tridimensional morphometric anatomical atlases from volumetric medical images (CT-Scan, MRI). This method allows automatic computation of a model by synthesizing a database of a given anatomical structure extracted from medical images of different patients. It operates by finding the features that are common to all the patients and computing their average position and a small set of statistical parameters describing their deformations.

What is particularly interesting is that no sophisticated a priori knowledge such as a sulci description or a cortical topography modelization [MRB+95] does need to be introduced. Moreover, no manual process is involved. We hope to obtain a model which takes into account the huge resolution of volumetric medical images (a MRI or CT-Scan image of the head composed of 200 slices of 256 by 256 pixels leads to a resolution of about 1 to 2 millimeters cube). Moreover, as we obtain morphometric parameters, we can envisage their usage in complex medical applications such as assisted diagnosis and therapy.

In previous articles, we have only presented work on a skull atlas and how it could be useful for studying a craniofacial deformity. In this paper, we will focus on a brain atlas. This is a very challenging problem because the cerebral shape is very variable but medical applications are numerous: anatomical or pathological study [RCJSG93] [TTP96], registration with functional data, assisted diagnosis [MPK94] or therapy planning.

In the first part of this paper, we briefly review each step of the atlas building method and we emphasize some specifics about the automatic construction of

an atlas of the brain. In the second part, we illustrate the relevance of this atlas by studying data from an individual patient. In particular, we show how it is possible to define "abnormal" deformations of the cerebral ventricles with a small set of parameters.

2 Construction of the brain atlas

The atlas construction method is composed of five steps (see Figure 1). We built the brain atlas from a database of 10 MRI brain images[1].

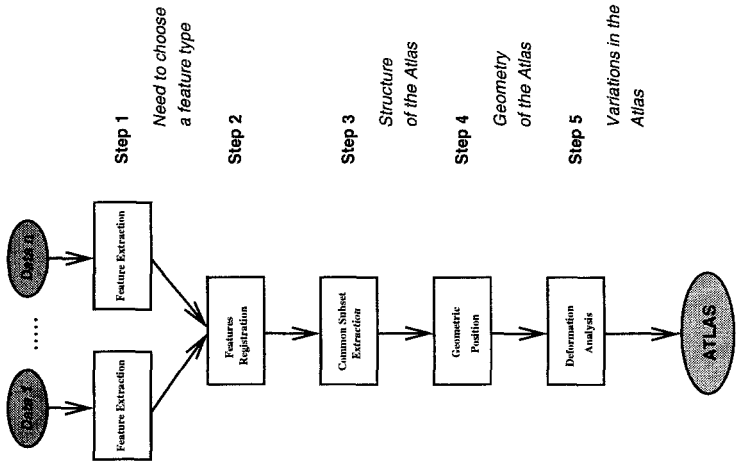

Figure 1. The proposed general scheme for automatically building anatomical atlases.

2.1 Step 1: feature extraction

A brief description. This step consists of automatically extracting 3D image features which will constitute the atlas. It is necessary to find a feature type which is both unambiguous definable (in order to be automatically computed) and anatomical relevant (in order to constitute a meaningful atlas). We choose "crest lines" [MBF92] whose points P are defined by:

$$\overrightarrow{\nabla} k_1 . \overrightarrow{t_1} = 0$$

where k_1 is the principal curvature which has the largest absolute magnitude and $\overrightarrow{t_1}$ the associated principal direction.

Using the "marching lines" algorithm [TG93], one can automatically extract the crest lines lying on a given isosurface directly from the volumetric image.

[1] These MRI data (referenced case1 ... case10) of resolution 123 slices of 256×256 pixels are courtesy of Dr. Ron Kikinis, Brigham & Women's Hospital and Harvard Medical School of Boston (United-States).

A simplified multi-scale scheme. As the mathematical definition of crest lines is based on a continuous description of a surface, it is necessary to convolve the discrete values of the image with a Gaussian function to obtain a continuous representation. The wider is the Gaussian parameter σ, the more regular the intensity is in the continuous representation. This smoothing leads to a modification of the position of the isosurfaces which support crest lines.

So, to obtain regular lines in a significant position, we propose to use a simplified multi-scale scheme:

- Extract a first set $\mathcal{S}_1$ of crest lines with a "low" Gaussian parameter.
- Extract a second set $\mathcal{S}_2$ of crest lines with a "high" Gaussian parameter.
- Register $\mathcal{S}_1$ and $\mathcal{S}_2$ by the line registration algorithm described in the next step "feature registration" and keep the lines of $\mathcal{S}_1$ which are matched with a line of $\mathcal{S}_2$.

This algorithm is quite crude because it uses only two values of the scale parameter and we are hopeful that more sophisticated multiscale methods will considerably improve the quality of crest lines.

In Figure 2, we show the results of the extraction of crest lines on the surface of the lateral cerebral ventricles. With a σ value set to 1.0, we obtain many lines (415) which appear quite noisy; whereas with $\sigma = 3.0$, we extract only 24 longer and smoother lines. However, in the second case, the crest lines do not follow the surface of the ventricles and we lose, in particular, a lot of information along the "horns" of the ventricles. After using the simplified multi-scale scheme, we obtain only 50 lines which seem significant and are precisely localized.

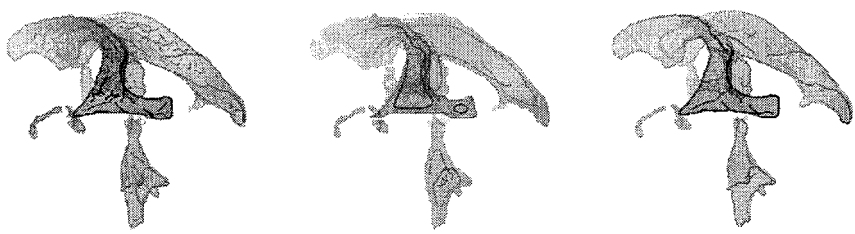

Figure 2. *Crest lines extracted on the surface of the lateral cerebral ventricles. Left, with a low Gaussian parameter,* $\sigma = 1.0$ *. Middle, with a high one,* $\sigma = 3.0$*. Right, after using a simplified multi-scale scheme.*

We apply this scheme to extract crest lines on the brain (see Figure 3). Notice that we also obtain lines inside along the cerebral ventricles.

An anatomical justification. By their mathematical definition, crest lines are localized along the salient parts of the surface. In particular, on the brain, they follow the convolutions and seem to match the anatomically defined patterns of gyri and sulci such as those referenced in the anatomical atlas [OKA90].

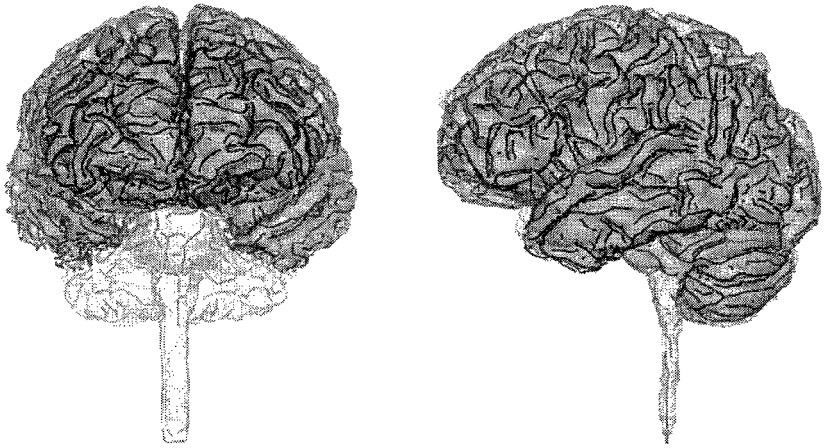

Figure 3. *Crest lines of the brain case1.*

2.2 Step 2: feature registration

A brief description. Given two sets of lines extracted from two different patients, we want a twofold result: line to line correspondences for the step 3 "common feature subset extraction" and point to point correspondences for the step 4 "feature average" and 5 "feature deformation analysis". For that purpose, we have adapted the "Iterative Closest Point" algorithm. We extend the original method by generalizing it to non-rigid deformations (affine and spline transformations) and applying it to lines (a line defines topological constraints over its points). For more details, the reader may refer to [STA95].

Separating sulci and gyri. For the registration process, we separate crest lines into two classes: those with positive "maximal" curvature and negative. Geometrically, this distinguishes crest lines which lie on a convex (the crown of the gyri) and concave surface (the fundi of the sulci).

In the registration algorithm, we separately find correspondences between gyral points and between sulcal points. Then, we use these two lists of matched points to compute a transformation which bring the two sets closer.

2.3 Step 3: common feature subset extraction

A brief description. From the registered lines, we are able to build a graph where each node represents a line of a set and each oriented link represents the relation "is registered with". Then, we can extract the bijective connected parts containing at least one line of each set: they represent the subsets of features which are common to all the data and which will constitute the structure of the atlas.

Some results. From the 10 brains, we found 82 subsets of lines which are present in each brain.

If the lines of one set have been labelled, it becomes possible to automatically label the subset to which they belong and then the corresponding common lines of the other nine sets.

We notice that even if crest lines of the brain are extremely variable, making the registration and graph construction processes difficult, the ventricles and medulla lines are correctly identified [Sub95].

2.4 Step 4: feature average

A brief description. It is necessary to find the mean positions of the features constituting the atlas (i.e., to average the sets of 3D lines defining each common subset).

First, we take a set of crest lines (for example, case1) as a reference set $\mathcal{R}$ and transform all the other sets into the reference frame using the rigid and isotropic scaling transformations computed from point to point correspondences found in step 2. Now, the remaining differences between lines represent meaningful morphological differences.

For each line $\mathcal{L}$ of $\mathcal{R}$, we find the deformations between $\mathcal{L}$ and the corresponding lines of the other sets. Then, we decompose them into a basis of fundamental deformations called modes by "modal analysis" [MPK94]. Once in this basis, the deformations are averaged and the "mean" deformation applied to $\mathcal{L}$ becomes the "mean" line. The set of these mean lines constitutes the atlas (Figure 4).

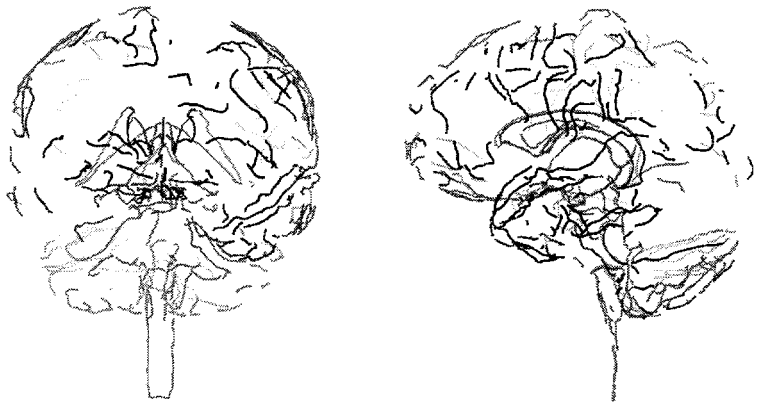

Figure 4. *The "mean" lines constituting the brain atlas. Notice the lines along the lateral ventricles.*

By using point correspondences between $\mathcal{R}$ and the atlas, we can find a volumetric spline transformation [DSTA95] and apply it to the surface of $\mathcal{R}$ in order to obtain a surface representation of the atlas.

2.5 Step 5: feature deformation analysis

A brief description. Let us assume that the the items of the database are "normal". In this step, we want to define the range of "normal" deformations which can be considered as the deformations between the atlas and the items.

We register the crest lines of the atlas with those of the database and we compute the modal decomposition of all these deformations. Then, for each line and for each mode i, we compute its average amplitude d_i and standard deviation σ_i.

If we register the crest lines of the atlas with the crest lines of a set S extracted from a patient image, we obtain also, for each line, some deformations decomposed in modes with the associated amplitudes $d^{Atlas,S}[i]$. We can then compare the modal amplitude $d^{Atlas,S}[i]$ with the "normal" modal amplitude by using an *amplitude distance* defined by (computed for the x, y and z axis);

$$dist(D^{Atlas,S}, i) = \sqrt{\frac{(d^{Atlas,S}[i] - d_i)^2}{\sigma_i^2}}$$

By using a χ^2 test, the larger values of $dist(D^{Atlas,S}, i)$ characterize the modes which are not in the average range and enable us to find the "abnormal" deformations.

3 Application to the study of cerebral ventricles shape

Introduction. In this section, we use the brain atlas to study an individual brain[2] $\mathcal{CE}$ in the following and, in particular, its cerebral lateral ventricles. Their deformations can be characteristic of Alzheimer's disease or hydrocephalus [MPK94].

First, we perform an automatic segmentation by mathematical morphology and thresholding tools to obtain the cortical surface presented in Figure 5, left.

Automatic labelling. We register the crest lines of the brain atlas with those of $\mathcal{CE}$. Then, we propagate the atlas labels to $\mathcal{CE}$ in order to identify some structures, in particular the lateral cerebral ventricles. In spite of the small number of atlas lines and the important geometrical differences between the atlas and the data, automatic labelling of the medulla, lateral ventricles and the first left lateral convolution appears visually correct in Figure 6.

Moreover, ventricles crest lines underline clearly the asymmetry of the ventricles with the left being much bigger than the right.

[2] MRI data of the head of resolution 254 slices of 256 × 256 pixels are courtesy of Dr. Neil Roberts, Magnetic Resonance Research Centre, University of Liverpool (Great-Britain).

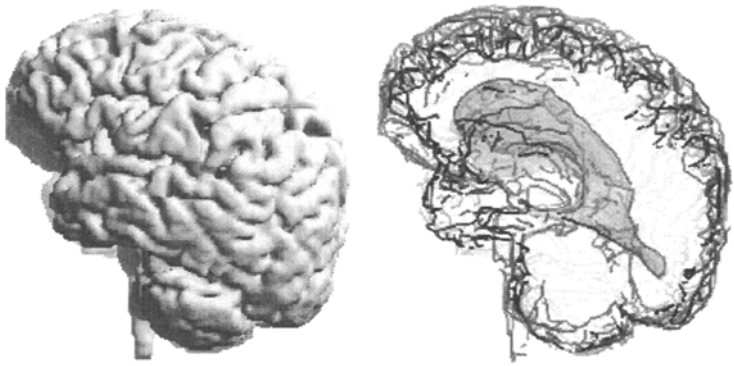

Figure 5. *Left: automatic segmentation of the cortical surface from a MRI of the head. Right: crest lines extracted on the cortical surface and the ventricles.*

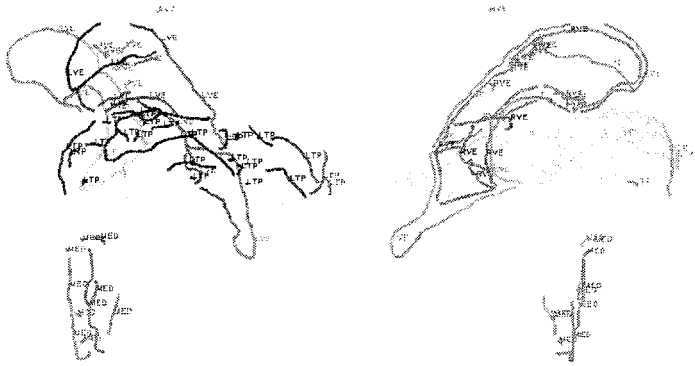

Figure 6. *Some lines of $\mathcal{CE}$ have been correctly labelled (medulla, left and right lateral ventricles, first left lateral convolution) thanks to the registration with the atlas.*

Qualitative study. By extracting the points of brain surface which are close to the ventricule crest lines, we can obtain the ventricle surfaces of the atlas and $\mathcal{CE}$. Moreover, from the matching of points found during line registration, we can apply a rigid and scaling transformation to $\mathcal{CE}$ in order to position it in the atlas frame.

In Figure 7, we can notice that not only the patient ventricles are asymmetric but they are also larger that the atlas ones.

Morphometric analysis. We can analyze the deformations of the longest atlas ventricular line. We decompose its deformation towards the correspondent patient ventricular lines and compute the amplitude distances for the first 5 modes.

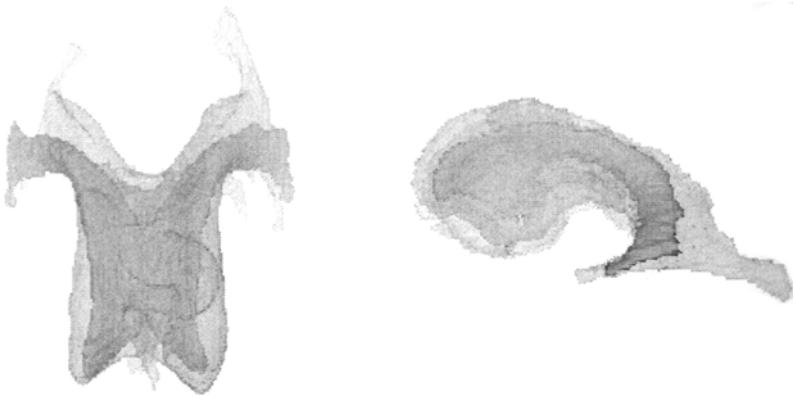

Figure 7. *Qualitative study of $C\mathcal{E}$ (in transparency) ventricles by superimposition wi those of the atlas (in solid).*

Significant deformations are those which are further than 3 standard deviatio from the average value for the x, y and z axis (see Table 1).

	Mode 0	Mode 1	Mode 2	Mode 3	Mode 4
Left x	-0.447	-5.125	+1.908	-2.140	-1.907
Right x	-1.026	+4.368	-2.254	+1.603	4.723
Left y	-3.687	+8.667	+0.451	+0.736	-5.081
Right y	-1.242	+8.336	-0.999	+0.757	-5.233
Left z	+4.429	-1.287	-3.731	-0.186	-1.442
Right z	+0.309	+1.824	-5.590	+1.986	-0.581

Table 1. *Amplitude distances for the 5 first modes of the deformation of the long left and right ventricular crest line deformation between $C\mathcal{E}$ and the atlas. The fram modes are detected as "abnormal".*

If we do not consider the mode 0 which corresponds to the translation, notice how "abnormal" modes tend to apply simultaneously to left and rig ventricles (with different amplitudes). It shows that both ventricles are "affecte by the deformations. The y and z "abnormal" modes have the same sign, they are oriented in the same sense. On the contrary, x "abnormal" modes ha opposite sign and the deformations are in inversed directions. If we only consic the first deformation mode which is the more global one, we notice that the x a y amplitudes are larger for the left ventricle. This confirms our visual analy that the two ventricles are asymmetric and that the left one is the largest.

Towards an assistance to diagnosis Now, let us study more specifically the three "abnormal" modes $1x$, $1y$ and $2z$. For that purpose, we apply successively to the atlas line these three modes and we visualize the results (see Figure 8). We can conclude that:

- the parameter $1x$ models the *horizontal curvature*,
- the parameter $1y$ measures the *vertical enlargement*,
- the parameter $2z$ quantifies the *longitudinal stretching*.

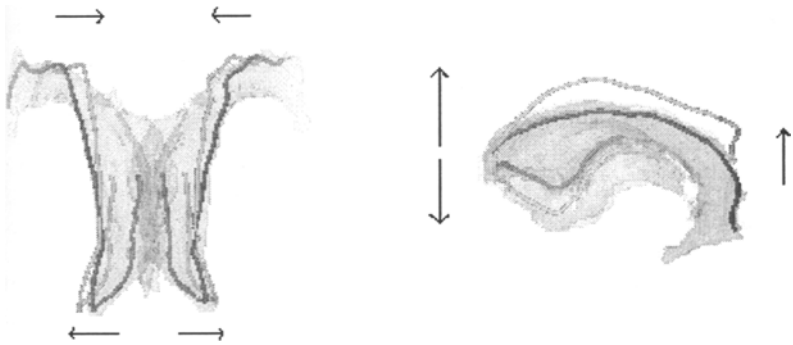

Figure 8. *Quantitative study of the ventricles deformation by analysis of the deformations and decomposition in "abnormal" modes ($1x$ and $1y$ modes). The atlas crest line is in black and the deformed one appears in grey.*

The amplitudes of these 3 modes could characterize the type and severity of deformations of the cerebral ventricles and hence automatically produce a diagnostic hypothesis based on a knowledge database.

4 Conclusion

In this paper, we have automatically built a simple 3D morphometric atlas of crest lines of the brain from 10 MRI images of different patients. We showed how this atlas could be used for some medical applications: automatic labelling, segmentation and assisted diagnosis.

We will concentrate our future work on four objectives:

- studying more precisely statistical tools for shape description: the Finite Element Method [MPK94], Principal Warps [Boo89], Fourier description [SKBG95], Principal Component Analysis [CTCG95].
- using other types of lines, for example, those based on 3D skeletonization [SBK+92].
- working on a larger database (several tens of items) in order better to take into account the variabilities of the human brain.
- validating our first results on a anatomical and medical basis, in particular, within the European Project BIOMORPH about the development and the validation of techniques for brain morphometry.

References

Boo89. F. L. Bookstein. Principal Warps: Thin-Plate Splines and the Decomposition of Deformations. *IEEE Transactions on Pattern Analysis and Machine Intelligence*, 11(6):567–585, June 1989.

CTCG95. T. F. Cootes, C. J. Taylor, D. H. Cooper, and J. Graham. Active Shape Models - Their Training and Application. *Computer Vision and Image Understanding*, 61(1):38–59, January 1995.

DSTA95. J. Declerck, G. Subsol, J.Ph. Thirion, and N. Ayache. Automatic retrieval of anatomical structures in 3D medical images. In N. Ayache, editor, *CVRMed'95*, volume 905 of *Lecture Notes in Computer Science*, pages 153–162, Nice (France), April 1995. Springer Verlag.

MBF92. O. Monga, S. Benayoun, and O. D. Faugeras. Using Partial Derivatives of 3D Images to Extract Typical Surface Features. In *CVPR*, 1992.

MRB+95. J.F. Mangin, J. Regis, I. Bloch, V. Frouin, Y. Samson, and J. Lopez-Krahe. A MRF Based Random Graph Modelling the Human Cortical Topography. In Nicholas Ayache, editor, *CVRMed'95*, volume 905 of *Lecture Notes in Computer Science*, pages 177–183, Nice (France), April 1995. Springer-Verlag.

MPK94. J. Martin, A. Pentland, and R. Kikinis. Shape Analysis of Brain Structures Using Physical and Experimental Modes. In *Computer Vision and Pattern Recognition*, pages 752–755, Seattle, Washington (USA), June 1994.

OKA90. M. Ono, S. Kubik, and Ch. D. Abernathey. *Atlas of the Cerebral Sulci.* Georg Thieme Verlag, 1990.

RCJSG93. J. Rademacher, V. S. Caviness Jr, H. Steinmetz, and A. M. Galaburda. Topographical Variation of the Human Primary Cortices: Implications for Neuroimaging, Brain Mapping, and Neurobiology. *Cerebral Cortex*, 3:313–329, August 1993.

SBK+92. G. Székely, Ch. Brechbühler, O. Kübler, R. Ogniewicz, and T. Budinger. Mapping the human cerebral cortex using 3D medial manifolds. In Richard A. Robb, editor, *Visualization in Biomedical Computing*, pages 130–144, Chapel Hill, North Carolina (USA), October 1992. SPIE.

SKBG95. G. Székely, A. Kelemen, Ch. Brechbühler, and G. Gerig. Segmentation of 3D Objects from MRI Volume Data Using Constrained Elastic Deformations of Flexible Fourier Surface Models. In N. Ayache, editor, *CVRMed'95*, volume 905 of *Lecture Notes in Computer Science*, pages 495–505, Nice (France), April 1995. Springer-Verlag.

STA95. G. Subsol, J.Ph. Thirion, and N. Ayache. A General Scheme for Automatically Building 3D Morphometric Anatomical Atlases: application to a Skull Atlas. In *Medical Robotics and Computer Assisted Surgery*, pages 226–233, Baltimore, Maryland (USA), November 1995.

Sub95. G. Subsol. *Construction automatique d'atlas anatomiques morphométriques à partir d'images médicales tridimensionnelles.* PhD thesis, Ecole Centrale Paris, December 1995. In French.

TG93. J.Ph. Thirion and A. Gourdon. The Marching Lines Algorithm : new results and proofs. Technical Report 1881, INRIA, March 1993. Available by anonymous ftp at ftp.inria.fr /INRIA/tech-reports/RR.

TTP96. A. W. Toga, P. Thompson, and B. A. Payne. *Development Neuroimaging: Mapping the Development of Brain and Behavior*, chapter Modeling Morphometric Changes of the Brain During Development. Academic Press, 1996.